

# Effect of Mg Addition on Solidification Structure of Low Carbon Steel

Kohichi ISOBE

Technical Development Bureau, Muroran R&D Lab., Nippon Steel Corporation, 12 Nakamachi, Muroran 050-8550 Japan.

(Received on April 21, 2010; accepted on July 23, 2010)

Effect of Mg addition on the solidification structure of low carbon steel containing about 0.1 mass% carbon was investigated in order to improve internal quality of cast blooms of this steel by some experiments using small size ingot casting. Some kinds of thermodynamic analyses on the crystallization of oxides and nitrides were also conducted along with FE-SEM observation on inclusions formed in cast ingots.

The results in this study were summarized as follows.

Adding Mg to the steel allows the equi-axed crystallization to be facilitated. In particular, the promotion effect is significant in low-carbon steel containing approximately 0.2–0.25 mass% Ti which leads to crystallizations of TiN until the end of solidification. The facilitating effect of equi-axed crystallization due to Mg addition in the steel without Ti content was presumably attributable to the heterogeneous nucleation by MgO or MgO·Al<sub>2</sub>O<sub>3</sub>, however, the facilitating degree is less compared with that in the steel containing Ti. It is apparent that MgO is also effective for TiN crystallization as the agent resulting in the significant promotion of heterogeneous nucleation of  $\delta$ -Fe and the equi-axed crystallization. Cooperative effect of MgO and TiN was confirmed in the low-carbon steel containing Ti by Mg addition. By Ca addition, the facilitating effect due to Mg addition is assumed to decrease to liquidize oxides and to reduce total oxygen, so that the crystallized amount of solid MgO or solid MgO·Al<sub>2</sub>O<sub>3</sub> decreases. It was verified that planar disregistry is a useful index to evaluate the relative heterogeneous nucleation capacity.

KEY WORDS: low carbon steel; Mg addition; heterogeneous nucleation; oxide; TiN; equi-axed crystallization; solidification; planar disregistry.

## 1. Introduction

Insufficient amount of equi-axed crystals in continuous casting of steel, occasionally provides the internal defects such as centerline segregation, center porosities and center cracks in cast blooms and slabs. These defects may not only deteriorate the properties of products but also decrease yield of products.

Technologies of low temperature casting<sup>1)</sup> and electromagnetic stirring<sup>2)</sup> have been developed to promote refinement of solidification structure. Specially, in the casting of about 0.1 mass% carbon steels and about 0.5 mass% carbon steels, the equi-axed crystallization is not enough to prevent the internal defects by applying those technologies.<sup>3)</sup> Productivity of curved mold type continuous caster in which equi-axed crystals easily sediment and pile in the lower side of strands, is typically lower due to the restriction of casting velocity because the defects have to be prevented in the casting of these steels.

This study aims at development of the promotion methods of equi-axed crystallization to improve the internal quality of cast blooms, focusing on the above mentioned background. The effects of Mg addition on the solidification structure of the low carbon steel containing about 0.1 mass% carbon, which would promote heterogeneous nucleation of  $\delta$ -Fe by inclusions formed by Mg addition,

were investigated.

## 2. Refinement Technologies of Solidification Structure by Promotion of Heterogeneous Nucleation and Problems of These Technologies

The refinement of solidification structure of steel has been investigated in previous studies.<sup>4-13)</sup> The results in these studies showed that the inclusions such as TiN, TiC, Ce<sub>2</sub>O<sub>3</sub>, MgO were effective for promotion of heterogeneous nucleation of bcc metals and the refinement of the metals and that MgO·Al<sub>2</sub>O<sub>3</sub> could facilitate TiN crystallization.<sup>4)</sup> Relationship between crystallographic coherency with  $\delta$ -Fe and capability of heterogeneous nucleation was studied and the studies clarified that materials having good coherency with nucleus tended to have high potency of heterogeneous nucleation.<sup>4-6)</sup> It has not been clarified how high facilitating effect is to obtain equi-axed crystallization of low carbon steel by the heterogeneous nucleating agents with good coherency with  $\delta$ -Fe.

In the actual application of heterogeneous nucleation, development of the methods of addition and dispersion of nucleus agents to molten steel was one of the challenges and it was required to take the effects on quality and properties of products and those on operation into account.

When the agents are added to molten steel to promote the

nucleation, it is not easy to disperse the agents to molten steel uniformly, because they easily float resulting in separation due to large difference in density between the agents and molten steel. Low wettability of the agents with molten steel also enhances the separation. A lot of inclusions remained in steel deteriorate fatigue strength and formability of products, even if the agents can be dispersed to the molten steel.

There are the methods in which the element such as Ti is added to molten steel to crystallize the nucleating agents such as TiN in molten steel. This application will be restricted, in the case where properties of products are greatly affected by large amount of the element addition necessary for the crystallization of nucleating agents. Mg addition was examined as one of the effective seeds for promoting the heterogeneous nucleation and the refinement of solidification structure in this study.

Therefore, the effects of Mg addition to two kinds of low carbon steels, with Ti and without Ti, were investigated in this study to prevent internal defects caused by lack of equi-axed crystals.

Amount of Mg addition necessary for nucleation was estimated by thermodynamic calculation model (SOLGAS-MIX<sup>14</sup>) on the crystallization behavior of MgO, MgO·Al<sub>2</sub>O<sub>3</sub> and other oxides before laboratory experiments. Then experiments were carried out by use of a vacuum induction melting (VIM) furnace by which 16 kg ingot was cast, to investigate the effect of Mg addition on solidification structure, based on the results of above analyses.

### 3. Promotion of Heterogeneous Nucleation by Mg Addition

Analysis by W. Kurz using classical nucleation theory has shown that the materials having small wetting angle with solidification nucleus, decrease the number of atoms and the activation energy necessary for nucleation.<sup>15</sup> As shown in Fig. 1, the lower interface energy with nucleus and the higher interface energy with liquid provides the

smaller wetting angle resulting in the high capability of heterogeneous nucleation. Estimation of the interface energy was carried out by measurements of supercooling on solidification<sup>9</sup>) or by First-principles calculation,<sup>16</sup>) but the estimation is very difficult.

The capability of heterogeneous nucleation is analyzed by use of planar disregistry<sup>6</sup>) defined in Eq. (1) in this crystallographic analyses about the capability of heterogeneous nucleation. This index has been proposed as a disregistry between two phases at the interface and it was reported that in general, the smaller the disregistry, the smaller supercooling was measured during solidification.<sup>5,6,17</sup>)

$$\delta_{(hkl)_n}^{(hkl)_s} = \sum_{i=1}^3 \frac{|(d[uvw]_s^i \cos\theta) - d[uvw]_n^i|}{d[uvw]_n^i} \times \frac{100}{3} \quad (\%) \dots(1)$$

where

- (hkl): a low-index plane
- [uvw]: a low-index direction in (hkl)
- d<sub>[uvw]</sub>: the interatomic spacing along [uvw]
- s: substrate
- n: nucleus ( $\delta$ -Fe)
- $\theta$ : the angle between the [uvw]<sub>s</sub> and [uvw]<sub>n</sub>

The planar disregistries between  $\delta$ -Fe or TiN and some kinds of compounds were estimated. The values of the disregistries between  $\delta$ -Fe and the following compounds; MgO, MgO·Al<sub>2</sub>O<sub>3</sub>, TiN, Ce<sub>2</sub>O<sub>3</sub> and Al<sub>2</sub>O<sub>3</sub> are listed in Table 1. Further, the values between TiN and the followings; MgO, MgO·Al<sub>2</sub>O<sub>3</sub> are also shown in Table 1. TiN, MgO and MgO·Al<sub>2</sub>O<sub>3</sub> have respective disregistries of 3.9, 2.8, 1.4% with  $\delta$ -Fe. MgO, MgO·Al<sub>2</sub>O<sub>3</sub>, these also have small disregistries of 1.1, 5.1% with TiN, respectively. Disregistries under 6%, are considered to be effective for heterogeneous nucleation.<sup>5</sup>)

The crystallographic relations above mentioned result in following anticipation as shown in Fig. 2. MgO and MgO·Al<sub>2</sub>O<sub>3</sub> inclusions probably help heterogeneous nucleation, when these are formed in molten steel by Mg addition. In the case where TiN crystallization is possible until

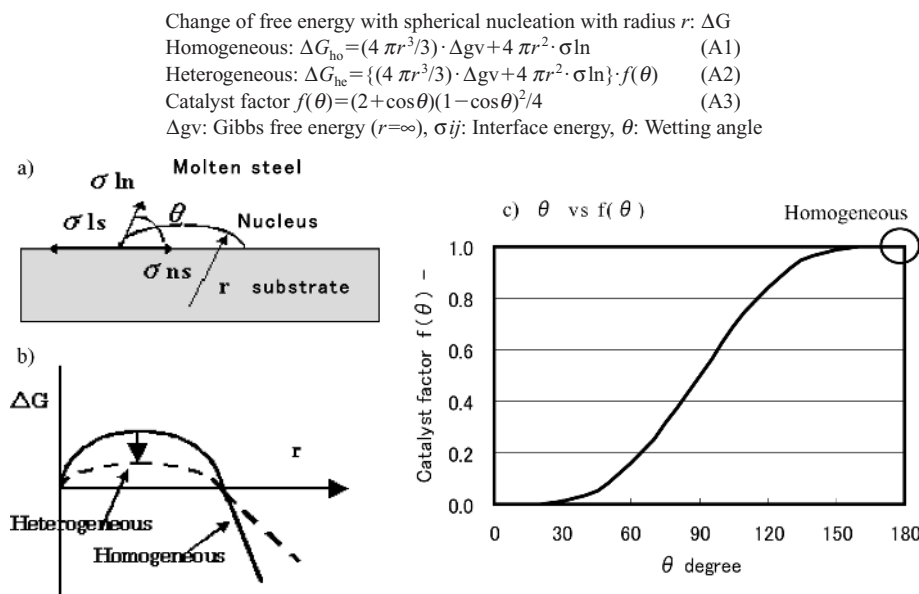
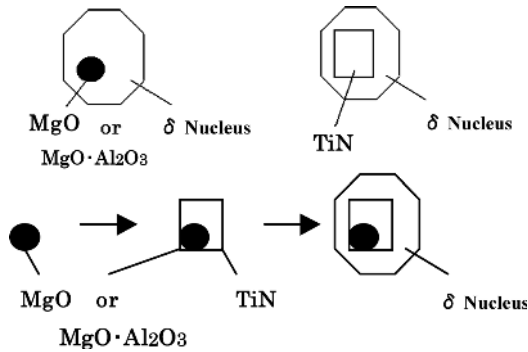


Fig. 1. Change of free energy with spherical nucleation with radius  $r$ .<sup>15</sup>)

**Table 1.** Planar disregistry between some materials and  $\delta$ -Fe or TiN.<sup>4-6)</sup>

| Material                           | vs $\delta$ -Fe | Material                           | vs TiN |
|------------------------------------|-----------------|------------------------------------|--------|
| MgO·Al <sub>2</sub> O <sub>3</sub> | 1.4 %           | MgO                                | 1.1 %  |
| MgO                                | 2.8             | MgO·Al <sub>2</sub> O <sub>3</sub> | 5.1    |
| TiN                                | 3.9             | Al <sub>2</sub> O <sub>3</sub>     | 11.7   |
| Ce <sub>2</sub> O <sub>3</sub>     | 4.1             |                                    |        |
| Al <sub>2</sub> O <sub>3</sub>     | 16.1            |                                    |        |



**Fig. 2.** Cooperation among some kinds of heterogeneous nucleation and chain of heterogeneous nucleation.

the end of solidification, it is expected that MgO, MgO·Al<sub>2</sub>O<sub>3</sub> inclusions promote the crystallization of TiN and, what's more, the crystallized TiN facilitates the heterogeneous nucleation of  $\delta$ -Fe with MgO, MgO·Al<sub>2</sub>O<sub>3</sub> inclusions. This is considered as a chain of heterogeneous nucleation.

**4. Analyses of Crystallization Behaviors of MgO, MgO·Al<sub>2</sub>O<sub>3</sub> and TiN**

The facilitation of heterogeneous nucleation of  $\delta$ -Fe is achieved by the existence of MgO, MgO·Al<sub>2</sub>O<sub>3</sub> and TiN in molten steel until the end of solidification.

The amount of Mg addition necessary for crystallization of MgO, MgO·Al<sub>2</sub>O<sub>3</sub> until the end of solidification, is analyzed by SOLGASMIX.<sup>14)</sup> This analyses focused on the relations between the amount of Mg addition and the kinds, the amount of crystallized oxides for the low carbon steel with representative chemical compositions shown in **Table 2**. The calculations using SOLGASMIX were carried out for the chemical compositions shown in Table 2 including oxygen content.

**Figure 3** and **Fig. 4** show the estimated relations between the amount of Mg addition and the crystallization behavior of oxides at 1500°C for steel A containing 0.25 mass% Ti and for steel B containing 0.2 mass% Ti, respectively. Ti<sub>2</sub>O<sub>3</sub> (S: solid) is formed by Mg addition lower than 5 mass ppm. Mg addition ranging approximately from 5 to 10 mass ppm forms liquid oxide mainly composed of Ti<sub>2</sub>O<sub>3</sub> and MgO. In addition, beyond about 8 mass ppm of Mg addition solid MgO forms, which is expected to promote heterogeneous nucleation as the nucleation sites. SOLGASMIX defines only Ti<sub>2</sub>O<sub>3</sub> as for Ti-O system, although the Ti-oxide formed actually under the present condition is Ti<sub>3</sub>O<sub>5</sub> referring to the previous study.<sup>18)</sup> **Figure 5** indicates the results analyzed by SOLGAMIX, on the kinds and the amount of

**Table 2.** Chemical compositions of test steels (mass%, mass ppm).

| Grade | C    | Si   | Mn   | P     | S     | T.Al  | Ti   | Nppm | T.Oppm |
|-------|------|------|------|-------|-------|-------|------|------|--------|
| A     | 0.05 | 0.80 | 1.65 | 0.010 | 0.011 | 0.008 | 0.25 | 35   | 20     |
| B     | 0.06 | 0.68 | 2.00 | 0.012 | 0.015 | 0.011 | 0.20 | 40   | 20     |
| C     | 0.11 | 0.01 | 1.25 | 0.015 | 0.007 | 0.031 | —    | 35   | 12     |
| D     | 0.10 | 0.01 | 0.32 | 0.014 | 0.020 | 0.033 | —    | 34   | 23     |

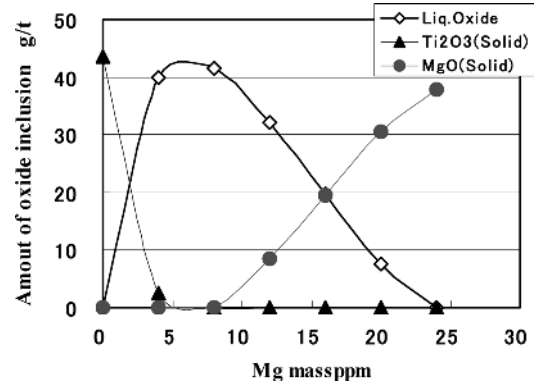


**Fig. 3.** Relationship between Mg content and amount of oxide inclusions (steel A, 1500°C).

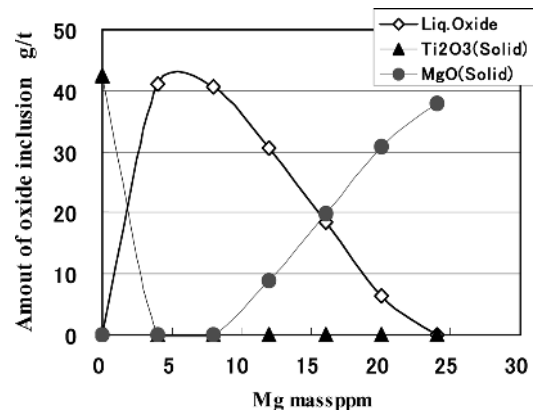


**Fig. 4.** Relationship between Mg content and amount of oxide inclusions (steel B, 1500°C).

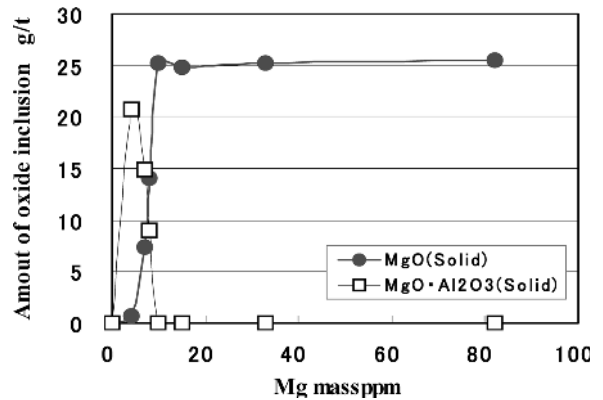


**Fig. 5.** Relationship between Mg content and amount of oxide inclusions (steel C, 1500°C).

equilibrium oxide inclusions formed in the low carbon steel without Ti at 1500°C. It is revealed that Mg addition up to 4 mass ppm mainly leads the formation of MgO·Al<sub>2</sub>O<sub>3</sub> with

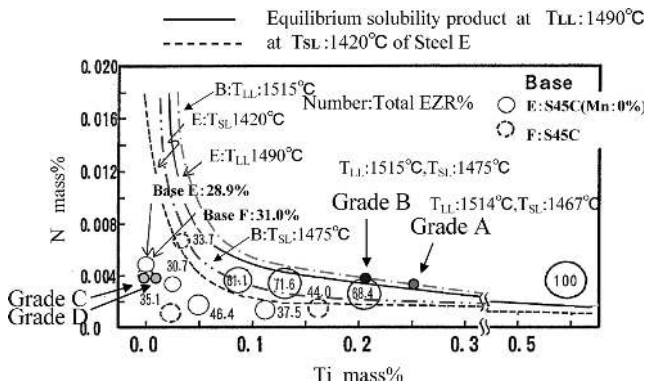


Fig. 6. Effect of TiN crystallization in molten steel on solidification structure.

little amount of MgO. The larger amount of  $\text{MgO} \cdot \text{Al}_2\text{O}_3$  than MgO is obvious up to 7 mass ppm Mg. Contrary, the amount of MgO exceeds that of  $\text{MgO} \cdot \text{Al}_2\text{O}_3$  at 8 mass ppm. Mg addition over 10 mass ppm brings the formation only of MgO.

The results of these analyses approximately agree with that calculated on the thermodynamic stable oxides for Fe–Al–Mg alloy by Ito *et al.*<sup>19)</sup> It was reported that the incorporation of 1 mass ppm Ca into molten steel containing Mg causes the liquidization of solid oxide such as MgO,  $\text{MgO} \cdot \text{Al}_2\text{O}_3$  in wide range of compositions of oxide in their investigation.<sup>19)</sup> Therefore, the effect of Ca was also investigated in this study, as the liquidization of MgO and  $\text{MgO} \cdot \text{Al}_2\text{O}_3$  seems to deprive the facilitating effect on the heterogeneous nucleation.

In addition, the behavior of TiN crystallization was examined by comparison with the previous studies<sup>11)</sup> in which the same experiments as those in this study were carried out. **Figure 6** shows the results of those experiments and the two curved lines in this figure indicate the equilibrium solubility limits of TiN estimated at liquidus temperature (1490°C: solid line) and solidus temperature (1420°C: broken line) of S45C (JIS) by use of the thermodynamic data recommended by JSPS the 19th Steelmaking Committee.<sup>20)</sup> The numbers and the size of circles in this figure show the equi-axed crystal zone ratio measured as area fraction for each case examined in the previous study. The center position of circle corresponds to the Ti and N contents in each case. It is apparent that the equi-axed crystallization is significantly facilitated in the case when Ti and N contents are over the TiN equilibrium solubility limit at solidus temperature implying that TiN crystallizes until the end of solidification.

TiN crystallization just upon liquidus temperature is most effective to have equi-axed crystal for welding whose solidification rate is high and solidification region is narrow.<sup>8)</sup> But TiN crystallized during solidification could facilitate the equi-axed crystallization and the equi-axed solidification progressed much more with increasing of the amount of TiN crystallization until end of solidification in those experiments. Much longer solidification time and the wider solidifying area in those than in the case of welding seems to provide opportunity of promotion of heterogeneous nucleation for crystallized TiN during solidification.

The respective liquidus temperatures of the steel A and B

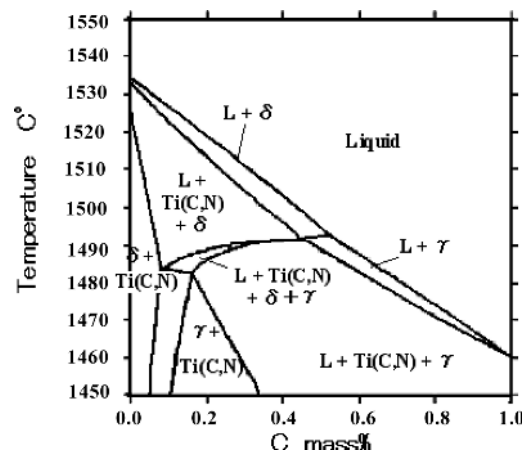


Fig. 7. Stable phase in Fe–C–0.2mass%Ti–40 mass ppm N estimated by Thermo-Calc.

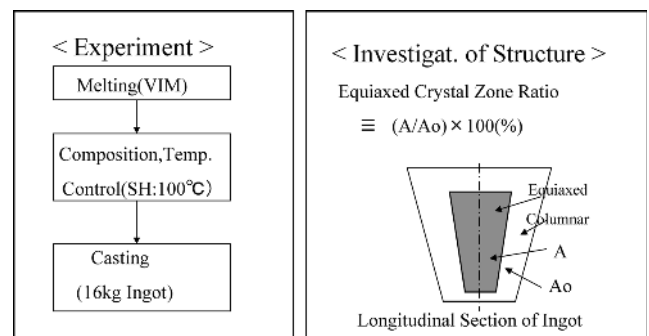


Fig. 8. Methods of laboratory experiments and investigation of solidification structure.

are 1515°C and 1514°C. The respective solidus temperatures of the steel A and B are 1475°C and 1467°C. The equilibrium solubility limits of TiN estimated at liquidus temperature (1515°C) and solidus temperature (1475°C) of steel B were also shown in Fig. 6. From the comparison of the points indicating Ti and N contents of steel A and B with these lines, it is expected that TiN may crystallize during solidification in steel A and B, if equilibrium state is achieved.

Furthermore, the behavior of TiN crystallization was analyzed by Thermo-Calc with the condition of 0.2 mass% Ti, 40 mass ppm N. Ti-nitride was defined as Ti(C,N), because the C content in Ti(C,N) is so small that Ti(C,N) is mostly equivalent to TiN. **Figure 7** shows that Ti(C,N) crystallizes within 10°C below the liquidus temperature. They may play a role as the site of heterogeneous nucleation.

## 5. Experimental Method and Procedure

Laboratory experiments were carried out in order to clarify how effective Mg addition was. Minimum amount of Mg addition necessary for the promotion of equi-axed crystallization is also focused on. The schematic view of the experimental procedure and the evaluation method of the ratio of equi-axed crystal zone is shown in **Fig. 8**. Sixteen kilogram ingots whose chemical compositions are shown in Table 2, were produced by the following procedure. The pure iron prepared electrolytically was melted in a vacuum-induction melting furnace (VIM) followed by addition of

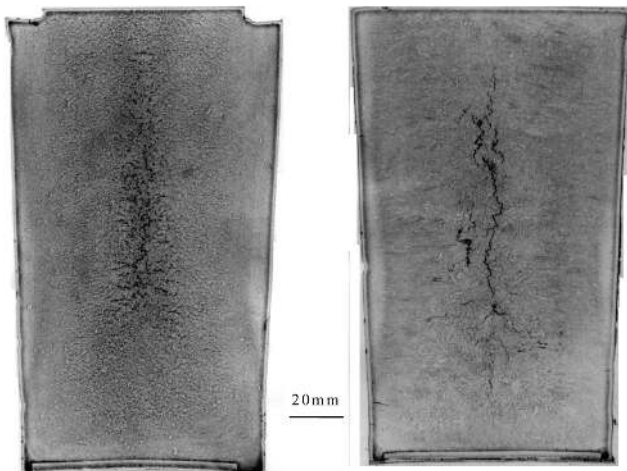
some kinds of alloy to adjust chemical compositions. After that, the molten steel whose superheat was controlled to about  $100 \pm 5^\circ\text{C}$  was poured into the mold made of cast iron.

To produce the ingots containing Mg, Fe–Si–Mg alloy was added to molten steel after the chemical compositions of molten steels except for Si and Mg were adjusted. In some of the experiments, Ca was added to molten steel with Mg to examine the effect of Ca addition. The amounts of Ti and N addition were increased in some experiments to investigate the effect of the increase in amount of TiN crystallization.

The chemical compositions of ingots were measured by chemical analyses of chips collected by drilling from the ingots. Etch prints (EP)<sup>21)</sup> were carried out at the longitudinal cross section of the ingots to evaluate the equi-axed crystal zone ratio (EZR). Specifically, the area of equi-axed crystal zone was measured by the use of EP and the EZR was calculated with dividing the area by the longitudinal cross-section area of ingot.

6. Experimental Results

Figure 9 shows EP prints of longitudinal cross section of



a) with 20 mass ppm Mg addition EZR: 66%  
b) without Mg addition EZR: 23%

Fig. 9. EP prints of longitudinal cross section of 16 kg ingots (steel A with 20 mass ppm Mg and without Mg).

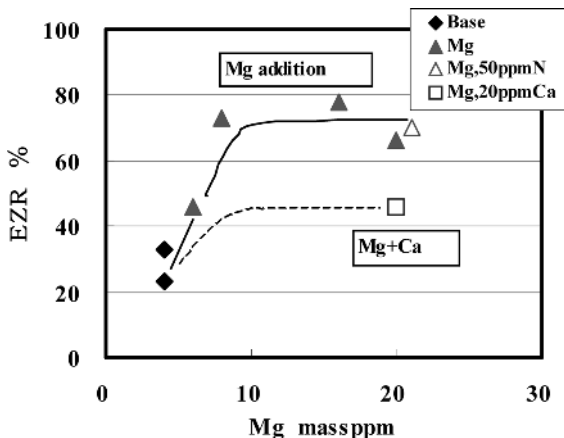


Fig. 10. Relationship between Mg content and EZR (steel A).

16 kg ingots of steel A. There is significant difference in equi-axed crystallization between those ingots. EZR of the ingot with 20 mass ppm Mg is 66% and large amount of fine granular equi-axed crystals are observed in this ingot. EZR of another ingot without Mg is 23% and coarse dendrite crystals are distributed in center part of the ingot.

Figure 10 shows the relationship between Mg content and EZR for steel A (0.25 mass% Ti) with TiN expected to form during solidification. The base steels also contained about 4 mass ppm Mg which might be attributed to contamination from the crucible of VIM.

The effect of promoting equi-axed crystallization is recognized from 5–6 mass ppm Mg above which Fe–Si–Mg alloy was added. The EZR increases with the increasing Mg content up to 10 mass ppm over which the effect is saturated.

For the plot of 20 mass ppm Ca, the EZR is clearly lower than without Ca addition. The decrease in heterogeneous nucleation sites due to the partial liquidization of solid oxides as expected in computation and decrease of total oxygen (T.O) from about 20 to 8 mass ppm probably causes this declination. The liquidization of oxides was confirmed that inclusions which have habit plane were decreased and spherical inclusions were increased in the ingot with Mg and Ca by SEM observation. The relationship between the T.O content and the EZR is shown in Fig. 11.

The relationship between the Ti content and the EZR is shown in Fig. 12. It should be noted that the effect of an increase of 0.1 mass% Ti on the increase in EZR by 50% is almost equivalent to very small amount of Mg addition of 8–20 mass ppm.

The results for steel B are shown in Figs. 13–15. Each figure shows the relationship between the Mg or T.O or Ti content and EZR. The results obtained for steel B were similar to those for steel A. The addition of only 8–20 mass ppm Mg provides the distinguished increasing in the EZR as the same degree as the addition of 0.08 mass% Ti. Both Ca and Mg addition also decreased the facilitating effects of the equi-axed crystallization by Mg addition in the steel B same as in steel A. In this case, the decrease in EZR by both Ca and Mg addition seems to be caused by decrease in heterogeneous nucleation sites due to reduction in T.O from about 20 to 8 mass ppm shown in Fig. 14. Clear

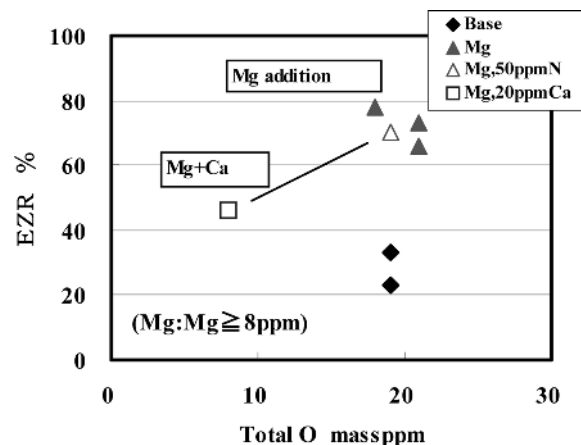


Fig. 11. Relationship between total oxygen content and EZR (steel A).

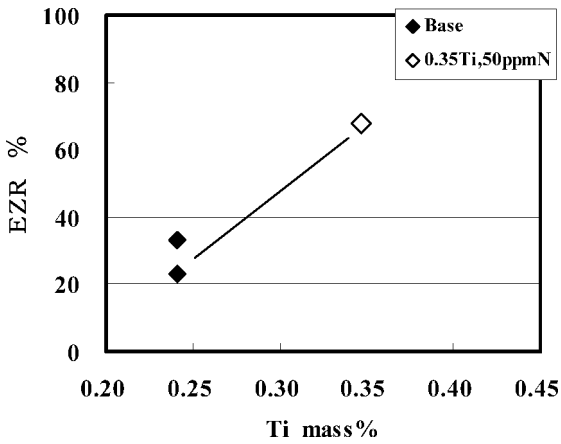


Fig. 12. Relationship between Ti content and EZR (steel A).

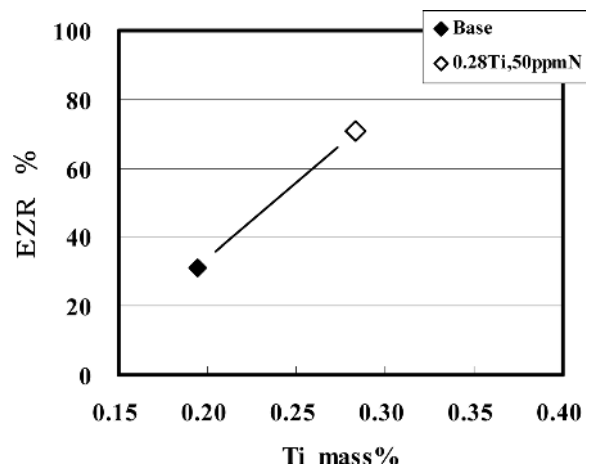


Fig. 15. Relationship between Ti content and EZR (steel B).

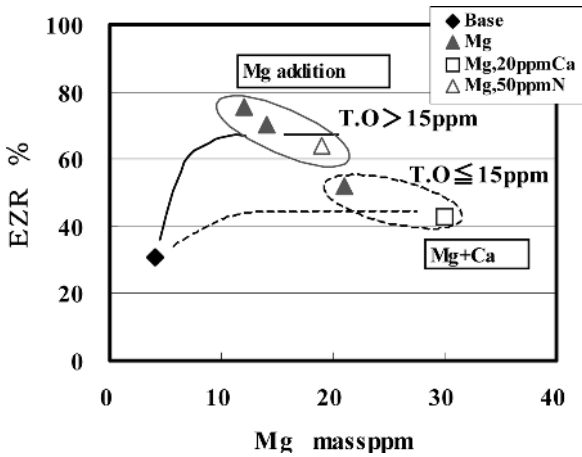


Fig. 13. Relationship between Mg content and EZR (steel B).

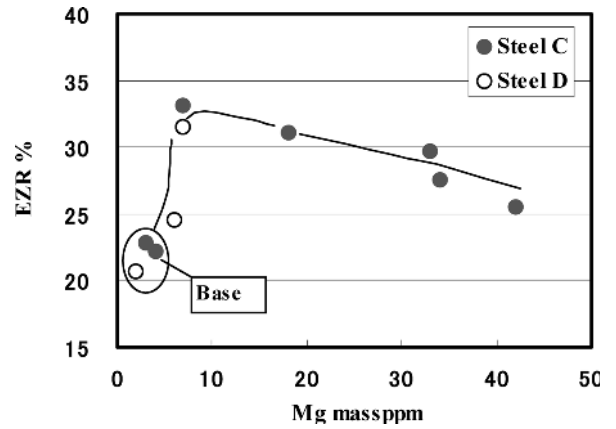


Fig. 16. Relationship between Mg content and EZR (steel C, D).

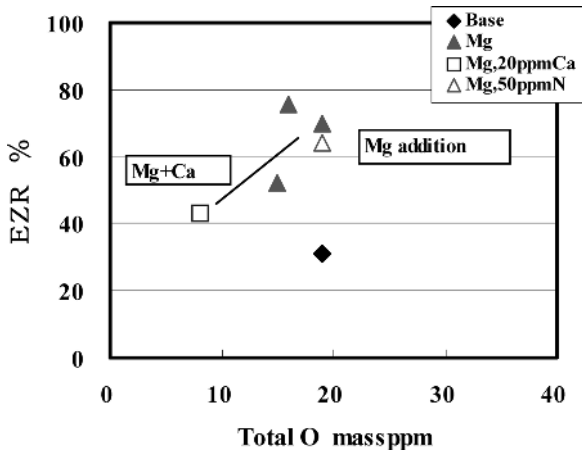


Fig. 14. Relationship between total oxygen content and EZR (steel B).

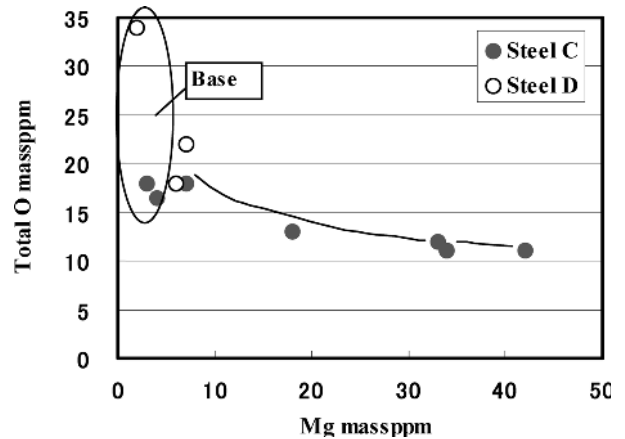


Fig. 17. Relationship between Mg content and total oxygen content (steel C, D).

evidence of liquidization of solid oxides was not obtained by SEM observation about inclusions in this case.

On the other hand, for steel grade C and D not containing Ti, 7–18 mas ppm Mg addition facilitated the equi-axed crystallization as shown in Fig. 16. The effect of increasing EZR from 21–24% of base steel to 31–33% was smaller than that for steel grade A and B.

The relationship between Mg content and T.O is shown Fig. 17. This figure shows that T.O is decreased with increase in Mg content in the case with Mg addition. The

comparison between Fig. 16 and Fig. 17 implies that larger amount of Mg addition leads to lower oxygen content according to deoxidation equilibrium. The fact brings the decrease in the amount of oxide inclusions probably resulting in the reduction in EZR.

The results above mentioned indicate that there is large difference between steel with and without TiN crystallization during solidification. More specifically, equi-axed crystallization of the steel grade with TiN crystallization, the equi-axed crystallization is extremely facilitated by small

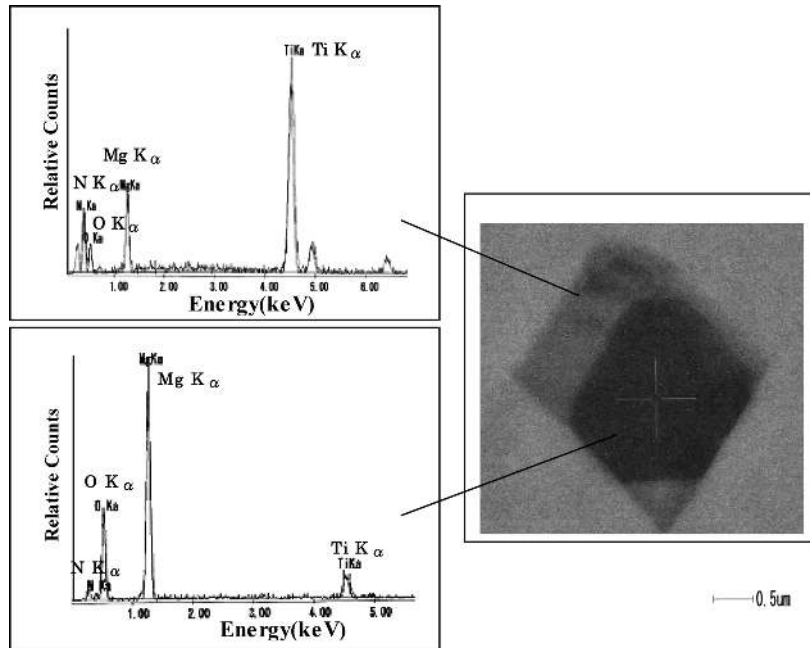


Fig. 18. FE-SEM back scattered image (compo image) and results of EDS analyses of representative inclusion (steel A).

amount of Mg addition.

### 7. Discussion

In this study, the existence of inclusions acting as the heterogeneous nucleation sites was examined to confirm the facilitating effects of Mg addition. Microscopic examinations using FE-SEM and EDS analyses were made for the samples extracted from the ingots.

Figure 18 shows the SEM compo images and the results of EDS analyses about the representative inclusions extracted from the ingots of steel A and B, in which the equiaxed crystallization was remarkably promoted by 7–18 mass ppm Mg addition. The part of inclusion recognized as oxides by back scattered electron (BSE) compo image, mainly consists of Mg and O, that is, the inclusion is MgO, on which TiN is crystallized. Although small amount of Ti is detected with small amount of N by EDS analysis in the part of oxide, this does not show the existence of Ti-oxide in the part, but probably seems to be effect of X-ray irradiated from TiN crystallized on the oxide, because of the small size of inclusions.

The results shown in this figure agree with those of analyses by SOLGASMIX. These also correspond to the results estimated about the behavior of heterogeneous nucleation of TiN, which is facilitated by MgO reflecting the good crystallographic coherency between TiN and MgO. In general, the behavior of equiaxed crystallization seems to depend on density of heterogeneous nucleation sites. Therefore, the density of MgO inclusions was estimated for the ingots of steel A with about 20 mass ppm Mg whose EZR were above 60%. This density was compared with density of equiaxed crystals in the center of ingot. The density of MgO inclusions was estimated from the T.O contents of the ingots that were about 20 mass ppm and the density of MgO (3.58 g/cm<sup>3</sup>).<sup>22)</sup> The density of MgO inclusions estimated was about 10<sup>4</sup>–10<sup>5</sup> order (number/cm<sup>3</sup>) on the assumption based on the SEM observation, that the diameter of MgO

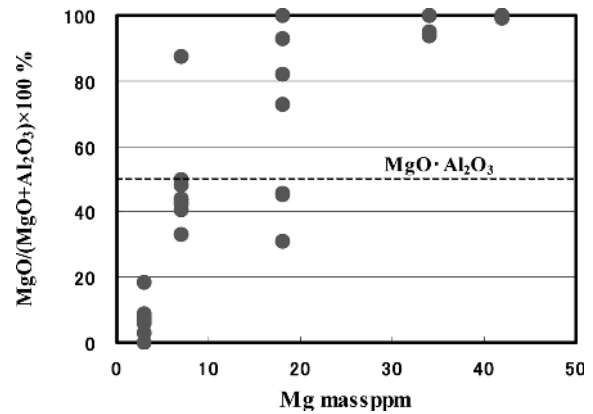


Fig. 19. Relationship between Mg content and MgO mole ratio in MgO–Al<sub>2</sub>O<sub>3</sub> oxide inclusions (steel C).

inclusion was 2–5 μm. This density approximately agree with the density of equiaxed crystals with diameter of 0.5–1 mm, which was estimated as 10<sup>3</sup>–10<sup>4</sup> order (number/cm<sup>3</sup>).

Figure 19 indicates the results of examination by use of FE-SEM and EDS analyses about the inclusions in the ingots of steel grade C and D which do not contain Ti and TiN. This figure indicates the relationship between Mg content and mole fraction of MgO in MgO–Al<sub>2</sub>O<sub>3</sub> system oxide. The composition of main oxide in the ingots containing 7 mass ppm Mg almost corresponded to MgO·Al<sub>2</sub>O<sub>3</sub>. Both MgO and MgO·Al<sub>2</sub>O<sub>3</sub> were recognized in the ingot having 18 mass ppm Mg. Only MgO was observed in the ingots containing Mg over 34 ppm. The comparison of Fig. 16 with Fig. 19 reveals that there is not distinguished difference in the facilitating effect of heterogeneous nucleation and equiaxed crystallization between MgO·Al<sub>2</sub>O<sub>3</sub> and MgO. One can understand that effect of inclusion population of these oxides is rather dominant than kinds of oxide as recognized from Figs. 16 and 17.

One can realize the following from the results shown in

Figs. 10, 12, 13, 15, 16 indicating the relationship between Mg or Ti content and EZR and the examination results on inclusions shown in Fig. 18 and Fig. 19. MgO and MgO·Al<sub>2</sub>O<sub>3</sub> crystallization in molten steel by Mg addition can provide facilitating the heterogeneous nucleation of  $\delta$ -Fe and the equi-axed crystallization. In addition, MgO formed by Mg addition promotes the TiN crystallization and the TiN contributes to the promotion of the heterogeneous nucleation and the equi-axed crystallization with MgO in the steels that have the possibility of TiN crystallization up to the end of solidification. If MgO·Al<sub>2</sub>O<sub>3</sub> is formed by Mg addition in the Ti containing steels, the same effects as MgO will be expected for the heterogeneous nucleation of  $\delta$ -Fe and TiN, because of the good coherency of MgO·Al<sub>2</sub>O<sub>3</sub> with  $\delta$ -Fe and TiN. The results of these examinations almost correspond to the results estimated previously.

The capability of heterogeneous nucleation by TiN was confirmed by measuring supercooling of molten steel<sup>5,10,17</sup> indicating the remarkable promotion effect of equi-axed crystallization observed in the several kinds of experiments including the previous studies.<sup>11</sup>) In addition, a previous study has provided the direct evidence showing that TiN behaved as the heterogeneous nucleation site for  $\delta$ -Fe.<sup>8</sup>) In the experiments of this study, the effect of facilitating the heterogeneous nucleation in steel A and B that have the possibility of TiN crystallization during solidification, is larger than that of steel C and D that have no possibility. This fact reveals that the facilitating capability of heterogeneous nucleation by TiN is larger than that by MgO or MgO·Al<sub>2</sub>O<sub>3</sub>.

By Fujimura *et al.*,<sup>4</sup>) it was confirmed that MgO·Al<sub>2</sub>O<sub>3</sub> facilitated the heterogeneous nucleation of TiN and the TiN crystallized on MgO·Al<sub>2</sub>O<sub>3</sub> promoted equi-axed crystallization of stainless steel by using liquid phase separation of Al–Mg–Ti complex oxides. But their study did not confirm the promotion of TiN crystallization by MgO and the facilitation of equi-axed crystallization by TiN crystallized on MgO. In addition, the effects of MgO and MgO·Al<sub>2</sub>O<sub>3</sub> on the heterogeneous nucleation of  $\delta$ -Fe were not recognized in their study.

From the results of this study, it was proved that TiN crystallization was facilitated by MgO and the crystallized TiN on MgO promoted equi-axed crystallization. These effects could be obtained by direct Mg addition to molten steel without using liquid phase separation of Al–Mg–Ti complex oxides. It was also confirmed that equi-axed crystallization could be promoted only by oxide inclusions of MgO or MgO·Al<sub>2</sub>O<sub>3</sub> without TiN crystallization, though the effect was even less than with TiN.

It was pointed that TiO related to the heterogeneous nucleation as nucleating agent and the facilitation of the equi-axed crystallization.<sup>23</sup>) Furthermore, it was also reported that the potency of heterogeneous nucleation by TiO and Ti<sub>2</sub>O<sub>3</sub> was large by measuring supercooling of molten steel on the substrate of these compounds.<sup>9</sup>)

The content of Ti in the experiments of this study is so small that the TiO formation is not probable.<sup>18</sup>) Ti oxides such as Ti<sub>3</sub>O<sub>5</sub> seem to form in the steel A and B when Mg is not added.<sup>18</sup>) But the degree of facilitating effect of equi-axed crystallization with Mg addition was larger than without Mg addition for these steels. These incorporated facts

prove that the facilitating effect of the heterogeneous nucleation by cooperation of MgO and TiN crystallized on MgO is larger than the individual effect of the above Ti oxides.

The results contrasting the behavior of equi-axed crystallization with the results by the analyses on the inclusions formed in the ingots approximately agreed with the tendency according to the coherency at the crystallographic planes evaluated by the planar disregistry. This result demonstrates that the planar disregistry is the effective index to evaluate the relative capability of heterogeneous nucleating agents.

## 8. Conclusions

The effects of Mg addition on the solidification structure of low carbon steel containing about 0.1 mass% carbon were investigated in order to find methods facilitating equi-axed crystallization for improvement of internal quality of cast blooms of this steel by some experiments using small size ingot casting. Some kinds of thermodynamic analyses on the crystallization of oxides and nitrides were also conducted along with FE-SEM analyses on inclusions formed in the cast ingots.

The main findings in this study are summarized as follows:

- (1) Adding Mg to low-carbon steel of 0.05–0.1 mass% C allows the equi-axed crystallization to be facilitated.
- (2) In particular, the promotion effect is significant in low-carbon steel containing approximately 0.2–0.25 mass% Ti by which TiN crystallizes until the end of solidification. In this steel, equi-axed crystallization is promoted even when the Ti content increases.
- (3) The facilitating effect of equi-axed crystallization due to Mg addition in the steel without Ti content is presumably attributable to the heterogeneous nucleation by MgO or MgO·Al<sub>2</sub>O<sub>3</sub>. However, the degree of facilitating effect is lower than the steel involving the crystallization of TiN.
- (4) The facilitating effect on equi-axed crystallization due to Mg addition in the low carbon steel containing approximately 0.2–0.25 mass% Ti can be explained as follows. Generated MgO inclusions facilitate the crystallization of TiN particles by heterogeneous nucleation which increase the heterogeneous nucleation sites for the solidification nucleus of  $\delta$ -ferrite. This mechanism tells us that MgO and TiN crystallized on MgO cooperatively promotes the heterogeneous nucleation of the solidification nucleus.
- (5) When both Ca and Mg are added, contrary, the facilitating effect of equi-axed crystallization due to Mg addition is reduced, because the amount of the heterogeneous nucleation sites are decreased by partial liquidizing of MgO, MgO·Al<sub>2</sub>O<sub>3</sub> and decrease in the amount of those oxides with reduction in T.O content.
- (6) It was verified that the planar disregistry was a useful index to evaluate the relative capacity as nucleating agents.

## REFERENCES

- 1) A. Suzuki: *Tetsu-to-Hagané*, **60** (1974), 774.
- 2) Y. Ujiie, H. Maede, Y. Ito, S. Ogibayashi, H. Seki, K. Wada and H. Ito: *Tetsu-to-Hagané*, **67** (1981), 1297.



- 3) R. Jauch, W. Courth, R. Heinrich, H.-P. Jang, H. Littersheit and E. Sowka: *Stahl Eisen*, **104** (1984), 429.
- 4) H. Fujimura, S. Tsuge, Y. Komizo and T. Nisizawa: *Tetsu-to-Hagané*, **87** (2001), 707.
- 5) B. L. Bramfitt: *Metall.Trans.*, **1** (1970), 1987.
- 6) T. Ohasi, T. Hiromoto, H. Fujii, Y. Nuri and K. Asano: *Tetsu-to-Hagané*, **62** (1976), 614.
- 7) Y. Ito, S. Shigeo, T. Okajima and K. Tashiro: *Tetsu-to-Hagané*, **66** (1980), 110.
- 8) T. Koseki and H. Inoue: *J. Jpn. Inst. Met.*, **65** (2001), 644.
- 9) T. Suzuki, J. Inoue and T. Koseki: *ISIJ Int.*, **47** (2007), 847.
- 10) K. Nakajima, H. Hasegawa, S. Khumkoa and S. Mizoguchi: *Metall. Mater. Trans. B*, **34B** (2003), 539.
- 11) K. Isobe, Y. Kusano and K. Hirabayashi: *CAMP-ISIJ*, **10** (1997), 973.
- 12) K. Isobe and Y. Kusano: *CAMP-ISIJ*, **15** (2002), 804.
- 13) T. Moroboshi, M. Zeze and T. Matsumiya: *CAMP-ISIJ*, **19** (2006), 746.
- 14) T. Matsumiya, W. Ymada, T. Koseki and Y. Ueshima: *Shinnittetsu Gihou*, **347** (1992), 68.
- 15) W. Kurz and D. J. Fisher: *Fundamentals of Solidification*, Trans Tech SA, Switzerland, (1984), 181.
- 16) T. Koseki, H. Kato, M. Tsutsumi, K. Kasai and J. Inoue: *Int. J. Mater. Res.*, **99** (2008), 347.
- 17) O. Grong: *Metallurgical Modeling of Welding*, The Institute of Materials, UK, (1997), 247.
- 18) W. Y. Cha, T. Miki, Y. Sasaki and M. Hino: *ISIJ Int.*, **46** (2006), 987.
- 19) H. Itoh, M. Hino and S. Banya: *Tetsu-to-Hagané*, **84** (1998), 85.
- 20) Report on Recommended Equilibrium Value of Reaction in Steelmaking, JSPS the 19th Steelmaking Committee, Tokyo, JSPS the 19th Steelmaking Committee-10588, (1984.11.6).
- 21) S. Kitamura, H. Miyamura, R. Isobe, K. Fukuoka and M. Hiari: *Tetsu-to-Hagané*, **68** (1982), S217.
- 22) R. Kiessling and N. Lange: *Non-metallic Inclusions in Steel* 2nd ed., The Metals Society, London, (1978), Part II, 6.
- 23) T. Nishizawa: *Bull. Iron Steel Inst. Jpn.*, **10** (2005), 583.